

# Cavitation induced by low-speed underwater impact

H. Kleine<sup>1</sup>, S. Tepper<sup>1</sup>, K. Takehara<sup>2</sup>, T.G. Etoh<sup>2</sup>, and K. Hiraki<sup>3</sup>

<sup>1</sup> *School of Aerospace, Civil, and Mechanical Engineering, University of New South Wales/Australian Defence Force Academy, Canberra, ACT 2600, Australia*

<sup>2</sup> *Department of Civil Engineering, Graduate School of Science and Engineering, Kinki University, Higashi-Osaka 577-8502, Japan*

<sup>3</sup> *Department of Mechanical and Control Engineering, Faculty of Engineering, Kyushu Institute of Technology, Kitakyushu, Fukuoka 804-8550, Japan*

## 1 Introduction

The subject of cavitation, that is, the formation and subsequent dynamics of voids within a liquid, has intrigued scientists for centuries, as can be readily seen from the large number of publications on this topic (comprehensive overviews are given, e.g., by Young or Lauterborn et al. [1, 2]). Hydrodynamic cavitation, which is found in fluid machinery or, more generally, in systems where the liquid is accelerated to high fluid velocities, is arguably the most obvious and possibly best known form of this phenomenon. Generally, voids in a liquid can be generated by the application of tension or through the localized deposit of energy [2]. Typically, tension is applied either through hydrodynamic forces in flowing systems (hydrodynamic cavitation) or through pressure and/or tension waves generated in a macroscopically static liquid (acoustic cavitation).

Cavitation can occur not only in technical systems but is also common in biology and medicine. Because of the often highly transient character of the life cycle of the voids within a liquid and their equally often diminutive size, this process is often only recognized with the help of special diagnostics. A recent example in which the (unexpected) existence and subsequently the importance of cavitation processes has only been found by using specialized high-speed photography is the investigation of the snapping shrimp [3].

The present investigation introduces a process of generating tension waves, which to the best of the authors' knowledge has not been reported before in the literature. The phenomenon described here was first discovered by Etoh and Takehara in 2004, when they were experimentally investigating the elasto-hydrodynamic rebound of rigid spheres in a liquid. Theoretical predictions of a low-pressure field and cavitation phenomena in the contact zone during the rebound had been made by Wells and Tsuji [4], and the original intention of the experiments was to determine the characteristics of this region. A new high-speed video camera developed by Etoh et al. [5, 6] and subsequently produced by Shimadzu under the name HPV-1 was the main diagnostic tool for these tests, in which a glass sphere was released under water to impact onto a glass plate (Fig. 1a). Typical drop heights were of the order of 200 mm and glass spheres with diameters between 15 mm and 25 mm were used. While the cavitation zone in the contact region was observed as expected, other cavitation phenomena in substantial distance to the contact zone were also seen (Fig. 1b). These observations led to the investigations described in the following.

Size and material of the spheres together with the drop height dictate that the maximum macroscopic flow velocity is of the order of 1 m/s and thus one order of magnitude below velocities at which hydrodynamic cavitation can be expected. It was initially assumed that jets out of the contact zone might be formed during the impact process and that locally the flow velocity might exceed the cavitation threshold. A series of

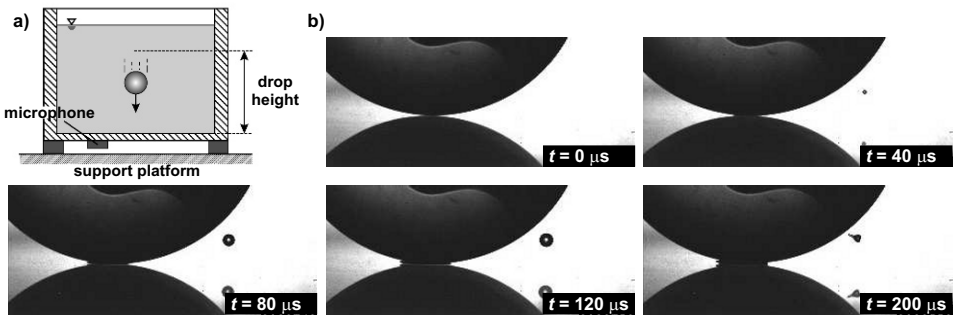


**Fig. 1.** a) Basic experimental set-up. The camera was triggered on the impact signal provided by the microphone. b) Underwater impact of a 20 mm dia. glass sphere on a glass plate in distilled water; impact speed approx. 1.5 m/s. Five frames of a shadowgraph sequence taken with 200 000 fps.  $t = 0$  is the instant of impact. Times indicated in the figure have an uncertainty of  $\pm 2 \mu\text{s}$ , however, time intervals between frames are correct within  $0.5 \mu\text{s}$ . The camera looked at an angle onto the plate, which leads to mirror images of the sphere and the cavitation bubbles.

preliminary Particle Image Velocimetry (PIV) tests showed, however, that the flow velocities around the sphere remained of the same order of magnitude as the drop velocity. Furthermore, the considerable distance of the bubbles to the contact zone makes hydrodynamic cavitation a less likely cause for the observed process.

Subsequently, it was hypothesized that tension waves caused by the impact be the responsible mechanism for the formation of the observed cavitation. Such waves mostly occur as the result of an inverted reflection of compression waves from an interface across which a substantial difference of acoustic impedance exists [7]. Arguably the most well-known process of this sort is an underwater explosion: the compression wave generated by the explosion (Fig. 2a) reflects as a tension wave at the water/air interface, while a pressure pulse is transmitted into the air. Large clusters of cavitation bubbles form below the water surface almost immediately behind the reflected expansion wave (Fig. 2c). In small-scale tests with charges of 10 mg silver azide, first bubbles occur within  $2 \mu\text{s}$  after the generation of the reflected expansion wave.



**Fig. 2.** Underwater explosion of 10 mg  $\text{AgN}_3$ . Three frames of a schlieren visualization sequence taken with 500 000 fps, time interval between shown frames  $\Delta t = 14 \mu\text{s}$ .

A similar mechanism can be identified in the case of the low-speed underwater impact of a sphere onto a plate to explain the observed cavitation phenomena outside of the contact zone. The impact at time  $t = 0$  generates pressure pulses within each partner of the collision (Fig. 3b). Please note that Fig. 3 is a highly simplified schematic that

only indicates the wave processes believed to be of major importance in this case. Waves that are transmitted into the liquid at the solid/liquid interface by pulses that propagate perpendicularly to the interface, for example, are not shown as their strength is believed to be insignificant. Furthermore, it was not attempted to depict the exact wave configuration within the sphere. Finally, waves caused by the presence of the accelerometer have not been indicated. Once the pressure pulses have reached the respective interfaces to the surrounding medium, namely the top of the sphere and the bottom of the plate, they are reflected as expansion waves. In the case of the plate (thickness  $d$ ) the reflection occurs at a time  $t_1 = d/a$ , where  $a$  is the sound speed within the plate. When this expansion wave again reaches the upper surface of the plate after a time  $t_2 = 2d/a$ , it propagates into the liquid, where it possibly interacts with the expansion wave generated by the sphere (Fig. 3d). This wave reflection process is repeated several times with ever diminishing amplitudes, but only the first reflection cycle is significant (hence all secondary reflected waves have been omitted in Fig. 3). The tension wave transmitted into the liquid then triggers the cavitation.

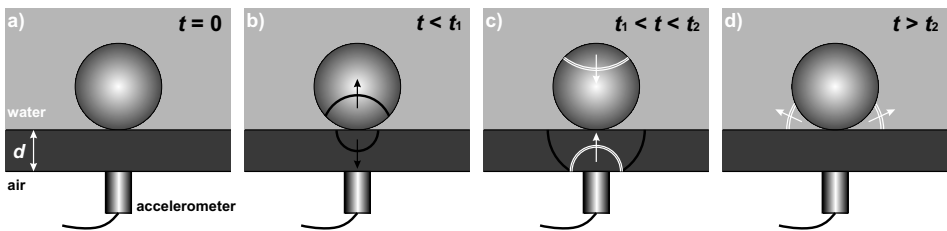


**Fig. 3.** Simplified schematic of the wave propagation as a result of an elastic collision between a sphere and a plate. **a)** Basic configuration at time of impact. **b)** Generation of pressure pulses in the plate and in the sphere. **c)** Reflection of expansion waves at the interface to medium of lower acoustic impedance. **d)** Resulting tension wave in the liquid.

If the lower side of the impact plate faces a medium of low acoustic impedance, such as sketched in Fig. 3, the reflection process occurs as described in straightforward fashion. If non-submersible transducers are mounted on the bottom as shown in Fig. 3a, such a configuration is automatically achieved. Should there be no substantial air gap between the impact plate and the platform on which the setup is resting (see Fig. 1a), i.e., should the impact plate be in direct contact with this platform, two different scenarios are possible:

- The acoustic impedance mismatch between the impact plate and the support platform is negligible: in this case, the generated pressure pulse would continue to propagate into the support platform. If this platform is of considerable thickness, the inverted reflection would either occur with significant delay or not at all, if the pressure pulse is attenuated in the platform material. In either case, the occurrence of cavitation through the described process is highly unlikely.
- A considerable mismatch in the acoustic impedance exists between the impact plate and the support platform. If the acoustic impedance of the support platform is lower, the reflection proceeds as described in Fig. 3. If it is higher (e.g., when a glass or plexiglass impact plate rests on an optical bench made of metal or granite), the pressure pulse will reflect without inversion at this interface. The inversion only occurs

when this reflected pulse reaches the plate/liquid interface, and it has to go through another reflection cycle before an expansion wave, at a time  $t_3 = 4d/a$ , propagates into the liquid. The cavitation-inducing tension wave is therefore both weaker and more delayed compared to the straightforward reflection case described above, and the resulting cavitation processes, with all other parameters kept constant, will be weaker or possibly not occurring at all.

While pure liquids without any form of contamination can withstand very high tensions without cavitating [7], the presence of contaminants, such as microscopic gas bubbles or minute solid particles, provides nuclei for cavitation and drastically lowers the cavitation threshold [1, 2, 7]. One would therefore expect different cavitation characteristics if liquids with clearly different contamination levels are used, such as distilled water and tap water. The tension wave in the liquid shown in Fig. 3d will therefore only then lead to the onset of cavitation, if it encounters an adequate nucleus.

## 2 Experiments

In the experimental campaigns that were conducted to investigate the observed cavitation phenomena, the following parameters were varied:

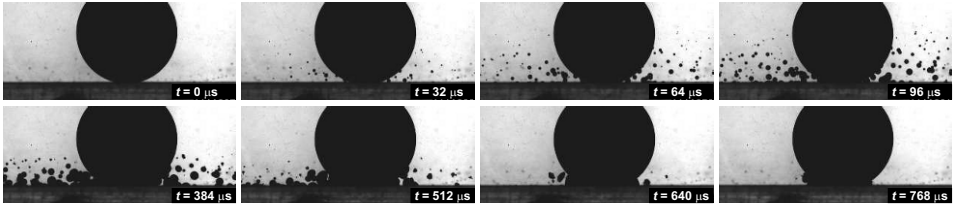
- drop height (from about 150 mm to 1 m);
- sphere size and material (19 mm to 30 mm; glass and stainless steel);
- contamination level of liquid (distilled water and tap water).

For larger drop heights the sphere had to be guided by a rod/rail system in order to achieve reproducible impact positions, while at smaller drop heights ( $\leq 200$  mm), the sphere was simply free-falling. An accelerometer (Briel and Kjaer Type 4366) was mounted at the bottom of the plate (as sketched in Fig. 3) to detect the arrival of the compression wave passing through the plate and to trigger the high-speed camera (analogous to a digital oscilloscope, the camera can be triggered on any of its hundred frames). Different high-magnification, high-sensitivity schlieren systems with schlieren head focal lengths between 6 m and 9 m were set up to visualize the waves generated by the impact. The camera was the aforementioned Shimadzu HPV-1, while illumination of about 1 ms duration was provided by a strong flash gun (Metz Mecablitz 45 CT-4). The flashlight was triggered by the sphere shortly before impact by interrupting a laser beam located about 2 mm above the plate. The system was synchronized in a way that the flash was approximately at its emission peak when the impact occurred. For direct observation of the impact and the bubble formation, a simple lens-based shadowgraph system was used, which for frame rates up to 125 000 fps could be run with a continuous light source. This system was also used to determine the speed and the acceleration of the sphere during the final 50 mm before impact. It was found that the speed did not exceed 2.7 m/s while acceleration levels within the visible test section were negligibly small – hence it is justified to assume that the sphere moves with constant velocity prior to the impact.

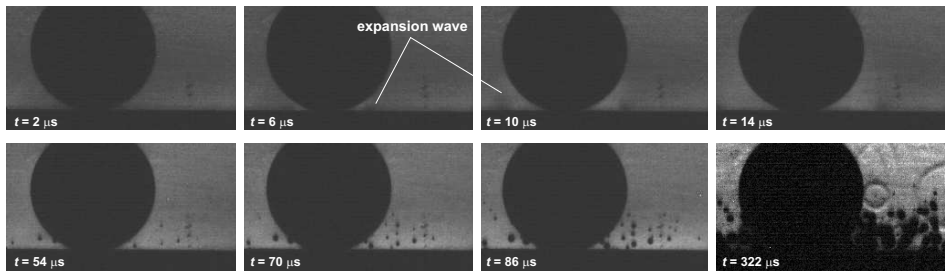
## 3 Results and discussion

Figure 4 shows frames of a sequence obtained by direct observation, similar to the frames shown in Fig. 1. In this case, the liquid was tap water. The considerably higher degree of

contamination becomes obvious through a significantly larger number of bubbles, which are produced throughout the whole field of view up to a height of about the sphere radius. Bubbles at larger vertical distances from the plate were only observed in less than 1% of all conducted trials.



**Fig. 4.** Underwater impact of a 25 mm dia. steel sphere on a 12 mm thick plexiglass plate in tap water; impact speed approx. 2.5 m/s. Eight frames of a shadowgraph sequence taken with 32 000 fps.  $t = 0$  is the instant of impact. Times indicated in the figure have an uncertainty of  $\pm 14 \mu\text{s}$  due to the low frame rate, however, relative time differences between frames are correct within  $2 \mu\text{s}$ . During the time interval covered by the shown frames, the steel sphere is essentially motionless. A recognizable rebound only occurs at about  $t \approx 800 \mu\text{s}$ , when the initial cavitation activity has terminated.



**Fig. 5.** Underwater impact of a 25 mm dia. steel sphere on a 12 mm thick plexiglass plate in tap water; impact speed approx. 2.5 m/s. Eight frames of a schlieren sequence taken with 250 000 fps.  $t = 0$  is the instant of impact. Times indicated in the figure have an uncertainty of  $\pm 1.5 \mu\text{s}$ , however, relative time differences between frames are correct within  $0.5 \mu\text{s}$ . In this experiment, bubbles become visible after approx.  $50 \mu\text{s}$  and begin to collapse about  $250 \mu\text{s}$  later.

Figure 5 shows a magnified view of the impact zone, taken with a higher frame rate and the schlieren system. In this trial, the camera recording was synchronized with the accelerometer. In the first row of Fig. 5, a wave is seen to emanate from the contact zone. As this is an expansion front, it is not as well defined as a shock wave and its appearance is clearer on the animated visualization than on single frames. In the given experiment, this wave occurs about  $5 \mu\text{s}$  after the accelerometer registers the impact. This time interval corresponds with sufficient accuracy to the time a pressure pulse needs to traverse the 12 mm thick plexiglass plate, if one assumes a sound speed of 2.6 km/s for plexiglass [8]. Within about  $50 \mu\text{s}$  after the wave has appeared, first cavitation bubbles become visible (second row, Fig. 5). For the given image resolution, the position of the sphere remains constant during the depicted time, which shows that the characteristic time of the

mechanical impact is orders of magnitude larger than that of the observed wave processes. This supports the assumption that hydrodynamic processes caused by the motion of the sphere have only a minor effect on the formation of cavitation. The generated bubbles undergo typical oscillations and form jets towards the sphere or towards each other, before eventually collapsing. The collapse generates spherical pressure pulses that are similar to blast waves (last frame of Fig. 5).

Tests with a thicker ground plate yielded essentially identical patterns, with the emanation of the expansion wave being delayed by the additional time the wave requires to traverse the thicker plate. The limited variation of drop height and sphere size and material has so far not revealed any obvious trends – cavitation has been seen even for the so far smallest sphere and lowest drop height. Preparations for tests in which the energy of the impact will be systematically varied to determine a threshold for cavitation onset in this test scenario are underway at the time of writing. So far, cavitation has been observed for impact energies around 100 mJ, which is orders of magnitude lower than what is typically found in laboratory-scale underwater explosions (such as the one shown in Fig. 2) or impact slugs such as those used by Trevena [7].

The influence of the expansion wave generated by the sphere is not fully clarified yet. All schlieren records show an emanating expansion wave that appears to be mainly generated within the plate. However, in a brief test series with a hemispherical impact body (in this case a cylinder with hemispherical tip), where the reflected expansion wave from the impact body would not exist or arrive significantly later, no cavitation was observed, although all other parameters were kept constant. This issue requires further studies, which in addition to shape variations of the impacting body will also include the use of materials with significantly different acoustic impedances.

## 4 Conclusions

The experimental evidence described here has so far supported the hypothesis that elastic waves generated during the impact are the responsible mechanism for the onset of cavitation in the presented low-speed underwater impact scenario. With the help of a newly developed high-speed video camera and a high-sensitivity schlieren system it was also possible to directly visualize the generated tension waves which are considered the cause of the subsequent formation of cavitation bubbles. The tests have also illustrated that considerable cavitation can exist in an environment in which at first sight one would not expect such a process. Impact energies of around 100 mJ have been shown to be sufficient for the generation of cavitation bubbles.

## References

1. Young FR: *Cavitation*. McGraw-Hill, London (1989)
2. Lauterborn W, Kurz T, Mettin R, Ohl CD: Adv. Chemical Physics **110**:295 (1999)
3. Versluis M, Schmitz B, von der Heydt A, Lohse D: Science **289**:2114 (2000)
4. Wells J, Tsuji Y: Proc. J.Soc. Multiphase Flow Meeting, Tsukuba (1994)
5. Etoh TG, Poggemann D, Ruckelshausen A et al.: Digest of Technical Papers, ISSCC 2002, pp.46-47 (2002)
6. Etoh TG, Poggemann D, Kreider G et al.: IEEE Trans. Electron. Dev. **50**(1):144 (2003)
7. Trevena DH: *Cavitation and tension in liquids*. Hilger, Bristol (1987)
8. Constantin C: Laser and Particle Beams **22**:59 (2003)